Particle Dispersion in Silica-Poly(vinyl alcohol) Coatings: Role of Particle-Polymer Interaction

Sunhyung Kim,[£] Sang Hoon Sung, Sanghyuk Lim, and Kyung Hyun Ahn*

Silica nanoparticle (SiNP)-poly(vinyl alcohol) (PVOH) coating is an important material system in paper coating applications, where particle distribution critically affects coating performance. In the present study, the authors investigated a role of physicochemical interaction between SiNP surface and PVOH chain in SiNP distribution in the coating layer, with a comparison of the suspension at pH 3 (good interaction) and pH 10 (poor interaction) as PVOH concentration was varied. Rheological properties and sedimentation behavior of the suspensions showed the dispersion stability of SiNP at pH 3 was improved by the addition of PVOH, whereas it was independent of the PVOH concentration at pH 10. Scanning electron microscopy and small angle x-ray scattering intensity of dried coating layer showed the uniform and dense structure with homogeneous distribution of SiNPs at pH 3, where spatial arrangement of SiNPs depended on the addition of PVOH. However, non-uniform and porous structures with SiNP aggregates were observed at pH 10, where the spatial arrangement of SiNPs was independent to the addition of PVOH. The stress development during drying of the coating suggested that the mechanical property was related to the spatial arrangement of individual SiNPs at pH 3, whereas to the distribution of SiNPs aggregates at pH 10.

Keywords: Silica nanoparticle-poly(vinyl alcohol)l coating; Particle-polymer interaction; Particle distribution; Dispersion stability; Rheology; Stress development during drying

*Contact information: School of Chemical and Biological Engineering, Institute of Chemical Process, Seoul National University, Seoul 151-744, Republic of Korea; *Corresponding author: ahnnet@snu.ac.kr*

[£]Present address: Corporate R&D, LG chem. Ltd, Republic of Korea

INTRODUCTION

Hybrid organic/inorganic coatings combine the flexible and ductile nature of the organic polymer with the rigid and thermo-mechanically stable nature of the inorganic particles. Silica nanoparticles (SiNPs) exhibit many advantages as an inorganic candidate because of low cost, high thermal and chemical stability, high abrasion resistance, and relatively low refractive index. Therefore, SiNP-polymer coatings have received much attention in applications such as adhesives, protective coating, optical coating, and barrier film (Zou *et al*. 2008; Ribeiro *et al*. 2014).

Poly(vinyl alcohol) (PVOH) is one of the most commercialized plastics in use due to its water-soluble and biodegradable properties and excellent mechanical properties as a barrier film and adhesive. By mixing with inorganic particles (*e.g.*, silica) or biomaterials (*e.g.*, cellulose), PVOH has been used in various applications, including paper coating as an ink-absorbing media (Zhang *et al*. 2015; Chen *et al*. 2017), protective coatings (Chang *et al*. 2015), electrolyte membranes (Yang *et al*. 2014), pharmaceutical coatings (Koo *et al.* 2011) bio-composites (Su *et al*. 2013), hydrogels (Tummala *et al*. 2016), and organic-

inorganic hybrid materials (Ching *et al*. 2015; Pingan *et al*. 2017).

Controlling the dispersion state of SiNPs in polymer matrix, as well as the resulting properties of the SiNP-polymer nanocomposite, has been intensively studied because the distribution of SiNP and its aggregates affect the material properties. One way to control SiNP dispersion is to adjust the physicochemical interaction between silica surface and polymer segment, for example, by selecting a suitable solvent (Bansal *et al*. 2005; Jouault *et al*. 2014) or varying the suspension pH (Kim *et al*. 2009). In aqueous SiNP/poly(vinyl alcohol) coatings, a physicochemical interaction between SiNP surface and polymer segment can be controlled by varying the suspension pH, which affects the hydrogen bonding between the silanol group of SiNP and the hydroxyl group in PVOH chain (Otsubo 1986). In a previous study on the SiNP-PVOH coating, the SiNP distribution was improved in SiNP-PVOH coating at low pH, resulting in increased PVOH adsorption on the SiNP surface (Kim *et al*. 2009).

Despite the importance of the particle-polymer interaction in particle distribution in SiNP-PVOH coatings, a fundamental understanding on the role of particle-polymer interaction in particle distribution, and resulting coating structure and property, is not yet fully understood. The role of particle-polymer interaction on structural evolution during drying and the resulting particle distribution in SiNP-PVOH coatings has been investigated previously (Kim *et al*. 2009, 2016; Lee *et al*. 2017). However, these studies were rather focused on the mechanism of drying behavior, and thus did not contribute much information on the property and structure of resulting dried coatings. Therefore, there has been a need to understand the structure and properties of the SiNP-PVOH coating resulted from varied particle-polymer interaction to obtain a controllable coating structure. It is particularly important in a paper coating application as an ink absorbing media, where porosity control is a key factor affecting product performance (Lamminmäki *et al*. 2012).

In the present study, the role of particle-polymer interaction in structure and property of a SiNP-PVOH coating was systemically investigated at a 'good' interaction and a 'poor' interaction by varying PVOH concentration in the suspension. First, the structure of the coating suspension was characterized by a sedimentation experiment and rheological measurement. Second, microstructure of the dried coating layer was probed at a particle and aggregate length scale by small angle x-ray scattering intensity and scanning electron microscopy (SEM) respectively. Finally, the mechanical property of coating layer was characterized by stress development measurement during drying. From the results, the dependency of structure and property of SiNP-PVOH coating was determined relative to ϕ_{PVOH} and exhibited a marked difference between the 'good' and 'poor' particle-polymer interaction.

EXPERIMENTAL

Materials

Charge-stabilized aqueous SiNP suspension (Ludox® HS-30, Aldrich, St. Louis, MO, USA) was used as received. The specific surface area of SiNP was 220 m^2/g, and the density was 2.2×10^3 kg/m^3 according to the supplier. From the SAXS measurement, average diameter of SiNP d was determined to be 15 nm, with $\sigma/d = 0.145$, where σ is the width parameter of the Schulz distribution function (Kim *et al.* 2013). The PVOH of molecular weight of 31×10^3 g/mol to 50×10^3 g/mol, degree of hydrolysis 87% to 88%, and

density of 1.19×10^3 kg/m^3, was supplied by Aldrich. A 15 wt.% PVOH solution was prepared as a stock solution by dissolving it in a deionized water at 80 °C for 3 h. The SiNP-PVOH suspensions were prepared to 10 wt.% of silica with a varied PVOH concentration(ϕ_{PVOH}) from ϕ_{PVOH} = 0.5 wt.% to 7.5 wt.%. Because pH of the suspension was initially pH 10, a 0.3 M HCl solution was gradually dropped into the suspension on the magnetic stirrer for the suspension pH 3. As time dependence was observed from the previous research (Kim *et al.* 2010), all measurements were performed for the suspensions of strictly 24 h stirring at room temperature.

Rheological Measurements

An ARES strain-controlled rotational rheometer (TA Instruments, New Castle, DE, USA) was used to investigate the rheological properties of the suspensions. Parallel plates geometry with 50 mm in diameter were used. The temperature was maintained at 25 °C during measurements by a Peltier system. A solvent trap was used to reduce evaporation during measurements. The steady shear viscosity of the suspensions was measured with 30 s of equilibration time and 30 s of measurement time. A frequency sweep measurement of the storage and loss moduli G' and G'' was conducted at a strain of 0.5%, which was within the linear viscoelastic regime obtained from the amplitude sweep test at the oscillatory frequency ω = 1 rad/s.

Coating Microstructure after Drying

The microstructure of the SINP-PVOH coating after drying was probed by small angle x-ray scattering (SAXS) and SEM (JSM-840A, JEOL, Akishima, Japan). SAXS measurements were performed on a PLS-II 9A U-SAXS beam line at the Pohang Accelerator Laboratory (Pohang, Korea). The two-dimensional (2D) scattering image from the sample of 0.1 mm thickness was recorded on a CCD detector (SX165, Rayonix, Evanston, USA). The wavelength of the x-ray beam was 1.1159 Å, and the sample-to-detector distance was 4511 mm, covering a range of 0.06 nm^{-1} to1 nm^{-1}.

Stress Development of Coating Layer During Drying

The cantilever deflection technique was utilized to measure stress development during drying of SiNP-PVOH coating (Payne *et al*. 1997). The cantilever made of a silicon wafer 70 mm long and 6 mm wide was clamped at one end with the other end free. After coating the suspension by blade coating applicator, the cantilever was brought to the drying chamber with a relative humidity of 10± 3% and drying temperature of 25±2°C for the measurement of cantilever deflection during drying. Deflection was measured by laser (LM-6501NAP, Lanics Co, Seoul, Korea) and position sensing detector (PSDM4, Thorlabs, USA) and recorded *in situ* during drying through a data acquisition system and program coded by LabVIEW (National Instruments, Austin, TX, USA). Deflection was transformed to stress using the Corcoran equation (Corcoran 1969). Details on the measurement equation can be found in Kim *et al*. (2009).

RESULTS AND DISCUSSION

SiNP-PVOH Interaction

The zeta potential (ζ) and adsorption amount of PVOH on the SiNP surface (Γ)

was evaluated by varying suspension pH, as shown in Fig.1 (Kim *et al.* 2016). A PVOH chain is adsorbed onto the SiNP surface by the hydrogen bonding of protonated silanol group (-SiOH) in SiNP and hydroxyl group (-OH) in PVOH chain. Protonation of the silanol group depends on suspension pH; *e.g.*, SiO^- is favorable in basic condition, whereas SiOH is favorable in acidic condition (Tadros 1978). Therefore, hydrogen bonding resulting in the increased amount of PVOH adsorption is promoted at the acidic condition. Therefore, the measurement of Γ allows for the quantification of the interaction between SiNP and PVOH, which depends on pH. Low Γ and the strongly negative ζ were measured at pH 10, which implied a poor SiNP-PVOH interaction. Low Γ was attributed to the ionized silanol group ($-SiO^-$) on the SiNP surface at the basic condition. As pH decreased, Γ increased by exhibiting a weakening of ζ, which suggested the protonation of the silanol groups (*i.e.* $SiO^- + H^+ \rightarrow SiOH$). As a result, pH 3 showed the largest Γ in the range of pH in this study, suggesting the best SiNP-PVOH interaction in the tested range of pH.

Based on the measurement of Γ, suspensions of pH 3 and pH 10 were selected as a representative 'good' interaction and 'poor' interaction, respectively, in this study. In the following section, the role of SiNP-PVOH interaction on dispersion stability, dried coating structure, and mechanical property was described by comparing pH 3 and pH 10.

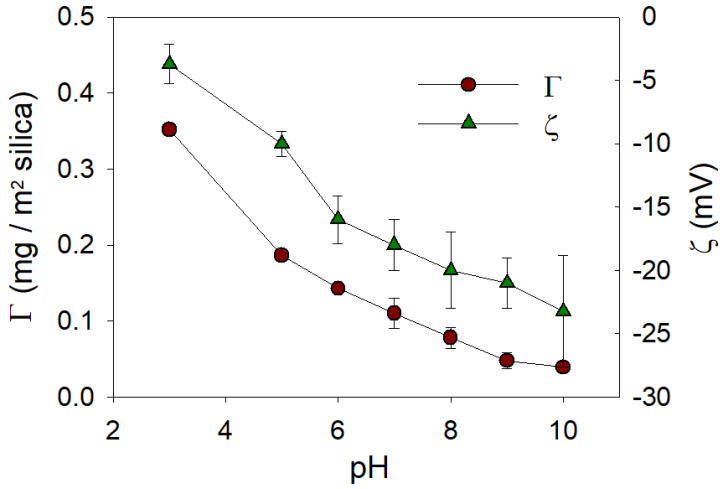

Fig. 1. Zeta potential of SiNP (ζ) and the amount of PVOH adsorption (Γ) as a function of suspension pH (Kim *et al.* 2016)

Sedimentation Behavior

Sedimentation behavior, which illustrates the effect of particle-polymer interaction on the dispersion stability, was evaluated for the SiNP/PVOH suspensions at pH 3 and 10. As shown in Fig. 2a, at pH 3 the sedimentation was fastest at ϕ_{PVOH} = 0.5 wt.%, but became slow as ϕ_{PVOH} increased. In a previous study about the Γ measurement as a function of ϕ_{PVOH} and the dispersion stability at pH 3, the authors found the dispersion stability improved as Γ increased, owing to steric stabilization as a result of adsorbed PVOH (Kim *et al*. 2015). The study showed that Γ increases as ϕ_{PVOH} increases, and the system approaches the plateau level at around ϕ_{PVOH} = 3 wt.%. Therefore, the improvement of sedimentation with increasing ϕ_{PVOH} in the range of 3.5 wt.% in Fig.2a can be understood by the steric stabilization because of increased Γ. When ϕ_{PVOH} increased above ϕ_{PVOH} = 3.5 wt.%, sedimentation was not observed any more, which suggested that the adsorption of

PVOH was fully saturated. However, it is notable that the suspensions at pH 3 showed a turbid image, which suggested that the SiNPs of 15 nm in diameter formed clustered structures in the suspension, where the length scale of the cluster was comparable to the wavelength of visible light; *i.e.* several hundred nm. In the previous study on the PVOH solution property at varied pH, the deterioration of PVOH chain was observed in a strongly acidic condition (Kim *et al.* 2009). However, neither a considerable turbidity change nor viscosity increase was observed as a signature of aggregation of the PVOH chain at a lower pH value. This suggests the deterioration of PVOH chain at least was not a dominant origin of the observed turbid image at pH 3. The cluster formation will be further discussed in terms of the rheological properties in the next section.

Sedimentation behavior at pH 10 was also evaluated in the range of ϕ_{PVOH} from 3.5 wt.% to 7.5 wt.%. Unlike the turbid image at pH 3, the suspension at pH 10 did not sediment, as shown in Fig. 2b. Furthermore, the suspension at pH 10 was nearly transparent, which implied that SiNPs at pH 10 do not form a clustered structure in the length scale of wavelength of visible light. This result was attributed to the charged nature of SiNPs at pH 10, which led the electrostatic stabilization of SiNPs in the suspension. In addition, the image at pH 10 did not change with the increased ϕ_{PVOH}, which implied that increased PVOH does not affect dispersion stability, probably owing to the poor interaction between SiNP and PVOH.

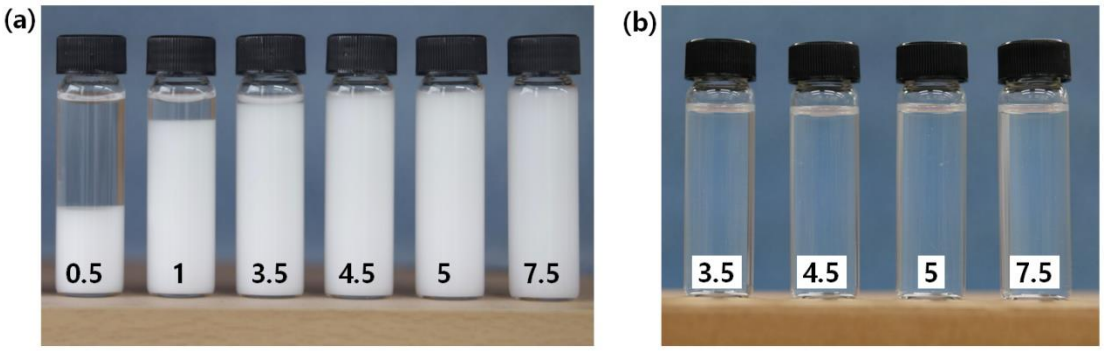

Fig. 2. Sedimentation image of 10 wt.% silica with a various ϕ_{PVOH} at pH 3(a) and pH 10(b)

Rheological Property

The steady shear viscosity (η) and the linear viscoelastic property of the SiNP-PVOH suspensions were measured at pH 3 and pH 10, respectively, to further understand the structure in the range of ϕ_{PVOH} between 3.5 wt.% and 7.5 wt.%.

At pH 3, strong shear thinning behavior was observed in the range of ϕ_{PVOH} from 3.5 wt.% to 5 wt.%, as shown in Fig. 3a. The shear thinning behavior in particle-polymer mixtures indicates particle cluster formation, which breaks down into a smaller cluster by shear flow, resulting in the reduced viscosity with increasing shear rate (Nasser *et al*. 2016). Therefore, the shear thinning behavior observed at ϕ_{PVOH} = 3.5 wt.% to 5 wt.% indicated that there was considerable formation of clusters. When ϕ_{PVOH} increased from 4.5 wt.% to 5 wt.%, viscosity decreased at the whole range of shear rate, and finally became a Newtonian fluid at ϕ_{PVOH} = 7.5 wt.%. This indicated that the cluster size reduced when ϕ_{PVOH} increased above 4.5 wt.% (Kim *et al*. 2015). The clustered structure was further characterized by the frequency sweep test. At ϕ_{PVOH} = 3.5 wt.% to 5wt.%, G' and G'' exhibited a power law behavior with a nearly equal slope, as shown in Fig. 3b and 3c. The

power law behavior with the same slope of G' and G'' can be seen elsewhere (Aoki *et al*. 2003), suggesting the formation of fractal-like particle clusters. This confirmed that there were clusters of SiNPs in ϕ_{PVOH} = 3.5wt.% to 5wt.%, as also supported by the turbid suspension images in Fig. 2a. When ϕ_{PVOH} increased up to 5wt.%, both G' and G'' decreased, which suggested a reduced size of clusters. Finally, the significant reduction of both G' and G'' was observed at ϕ_{PVOH} = 7.5 wt.%, which implied reduced cluster size. The cluster formation probed by rheological measurement could be further understood by the measurement of a small angle x-ray scattering and a small angle light scattering intensity for SiNP-PVOH suspension of pH 3 (Kim *et al*. 2015). The scattering intensity showed the formation of SiNP clusters were mainly dominated by depletion flocculation below ϕ_{PVOH} = 4 wt.%, whereas it was dominated by depletion stabilization above ϕ_{PVOH} = 4wt.%. On the basis of this study, the power law behavior of G' and G'' at ϕ_{PVOH} = 3.5 wt.% to 5wt.% was attributed to depletion clustering, and the serious reduction of G' and G'' at ϕ_{PVOH}= 7.5 wt.% was a signature of depletion stabilization.

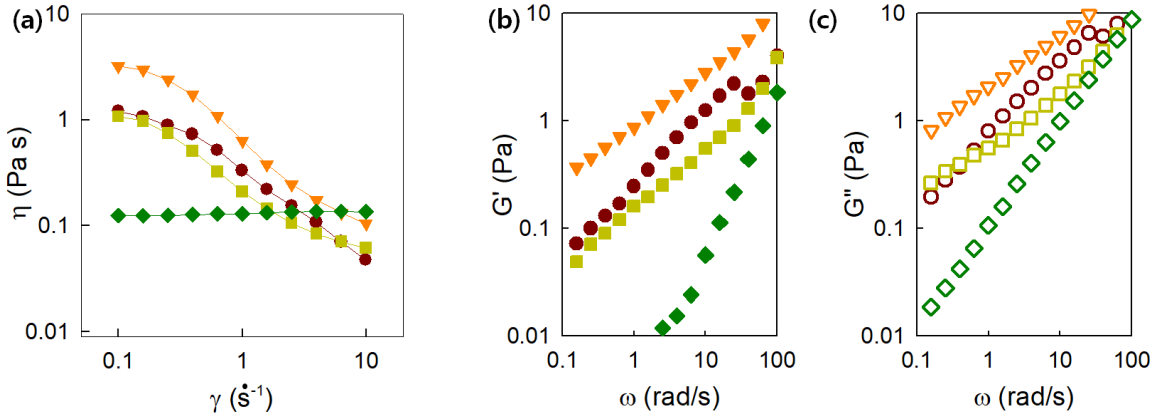

Fig. 3. (a) Steady shear viscosity curve and (b, c) frequency sweep measurement results of G' and G'' for the SiNP-PVOH suspension at pH 3 by varying ϕ_{PVOH}. ϕ_{PVOH}= 3.5(●, ○), 4.5 (▼▽), 5 (■, □), 7.5 (◆, ◇) (by wt.%)

The rheological property of the suspension at pH 10 is displayed in Fig. 4.

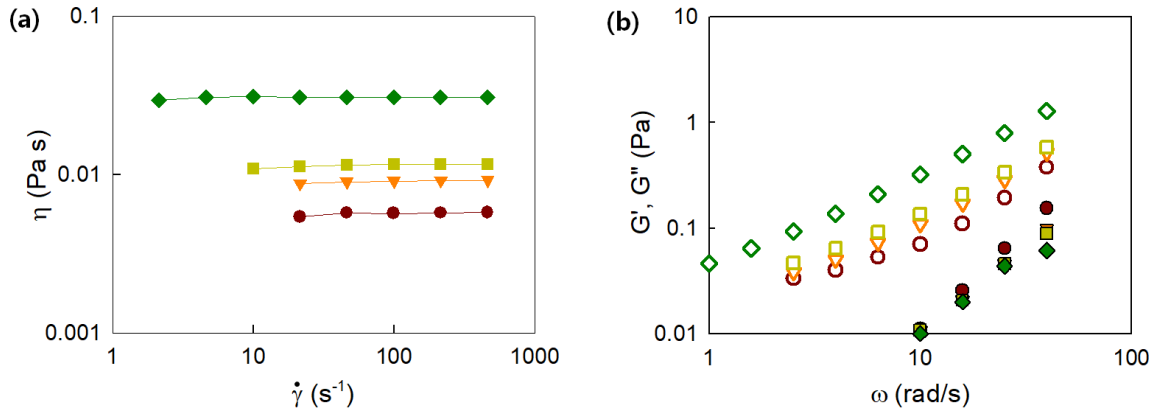

Fig. 4. (a) Steady shear viscosity curve and (b, c) frequency sweep measurement results of G' and G'' for the SiNP-PVOH suspension at pH 10 by varying ϕ_{PVOH}. ϕ_{PVOH} = 3.5(●, ○), 4.5 (▼▽), 5 (■, □), 7.5 (◆, ◇) (by wt.%)

Unlike the shear thinning behavior at pH 3, which significantly depended on ϕ_{PVOH}, the viscosity curves at pH 10 exhibited Newtonian behavior, which was independent of ϕ_{PVOH}, as shown in Fig. 4a. The Newtonian behavior was observed in a stable suspension with a good dispersion, where there is no formation of particle clusters which breakdown by shear flow, even at high shear rates (Di Giuseppe *et al.* 2012). Therefore, the observed Newtonian behavior in Fig. 4a suggested that charged SiNPs do not form clusters at pH 10, as supported by transparent images in Fig. 2b. In the frequency sweep test, G' was negligibly small as shown in Fig. 4b, which indicated that there was no considerable aggregated structure. G'' increased in the order of increased ϕ_{PVOH}, which suggested the contribution of increased PVOH in the medium.

Microstructure of the Silica/PVOH Coatings after Drying

The structure of the dried SiNP-PVOH coating was investigated by means of SEM and SAXS. The authors previously studied the structure of dried silica-PVOH coating at a limited ϕ_{PVOH} between 4 wt.% and 5 wt.% (Kim *et al.* 2016). To further understand the effect of ϕ_{PVOH} on the coating structure, here the silica-PVOH coating was tested over a wider range of ϕ_{PVOH} from 3.5 wt.% to 7.5 wt.%. SEM images of the dried coating layer at pH 3 and pH 10 are shown in Fig. 5. A uniform and dense structure with unobservable aggregates was clearly seen for pH 3 within the whole ϕ_{PVOH} range under the investigation (Fig. 5a), whereas non-uniform and porous structure with large aggregates was observed at pH 10 (Fig.5b). The SEM image did not show a dependency of ϕ_{PVOH} at pH 3, but showed a strong dependency on ϕ_{PVOH} at pH 10; *i.e.* pores gradually reduced as ϕ_{PVOH} increased, and finally disappeared at ϕ_{PVOH} = 7.5 wt.%, with the aggregates which became considerably small.

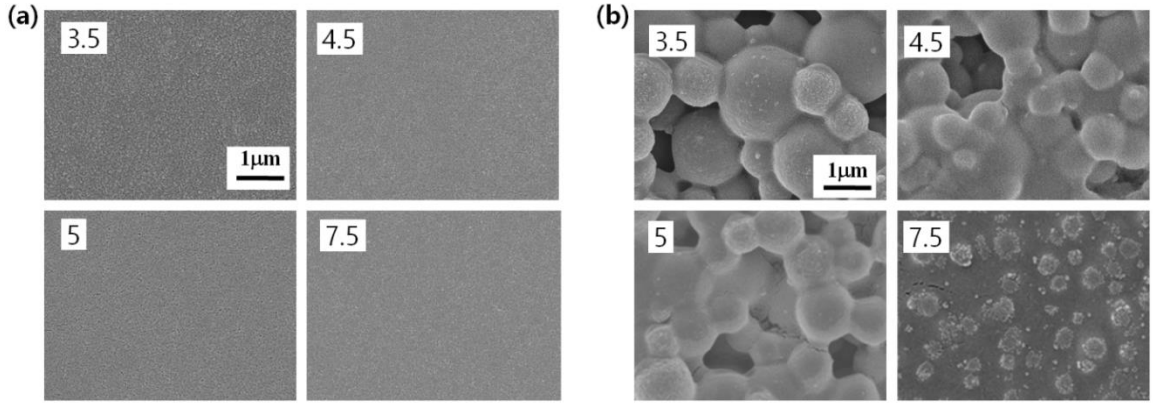

Fig. 5. Scanning electron microscopy image of silica/PVOH coating surface after drying at (a) pH3 (b) pH 10 as a function of ϕ_{PVOH}. The coatings were prepared from the aqueous 10 wt.% silica suspensions with varying PVOH concentration (wt.%, noted in the figure).

The SAXS technique was employed to characterize the structure of the coating film in Fig.6 at the particle length scale. This technique provided the information on the spatial organization of SiNPs in the film at the particle length scale, which clarified the relative position of the SiNP and PVOH in the dried coating film because of SiNP-PVOH interaction.

A broad peak at around q = 0.39 nm^{-1} was observed at pH 3, as can be seen in Fig. 6a.The peak position at q = 0.39 nm^{-1} allowed for calculation of the center-to-center

distance between neighboring SiNPs *h* through $h = 2\pi/q$, which yielded h = 16.1 nm. This was slightly larger than the diameter of SiNP, d=15nm (Kim *et al*. 2013), which suggested the presence of PVOH and the accompanying bound water (Hatakeyama *et al.* 1987) between SiNPs. The broad peak indicated that the particles in the film were loosely arranged, where PVOH was well-mixed with SiNPs. The broad peak became wider with the slight increase in the low q intensity as ϕ_{PVOH} increased, finally disappeared at ϕ_{PVOH} = 7.5 wt.%. This can be understood as a gradual disappearance of SiNP arrangement because SiNPs became far apart from each other with increased PVOH, as a result of a favorable mixing with PVOH in the solid film (Kim *et al.* 2016).

SAXS intensity at pH 10 showed a marked distinction from that at pH 3. Upturn at the lowest q and a shoulder at q = 0.43 $nm^{-1}$was observed in SAXS intensity of pH 10, as shown in Fig.6b, which suggested that the particles formed disordered aggregates. The center-to-center distance between SiNPs h was calculated to 14.6 nm from the shoulder at q = 0.43 nm^{-1}, nearly the same as the SiNP diameter. This implied that the aggregates shown in the SEM image (Fig.5b) were formed by the contact of bare SiNPs, in the absence of PVOHs inside the aggregates. Furthermore, the peak position at pH 10 did not shift with increasing $\phi_{PVOH,}$ indicating that the increasing ϕ_{PVOH} did not affect the SiNP structure in the aggregates. In conclusion, the location of PVOH observed in the SEM image (Fig.5b) and aggregate structure of SiNPs seen in SAXS intensity suggested that PVOH stayed outside of the SiNPs aggregates and did not play a role in improving SiNP distribution at pH 10, owing to the poor interaction between SiNP and PVOH (Kim *et al*. 2016).

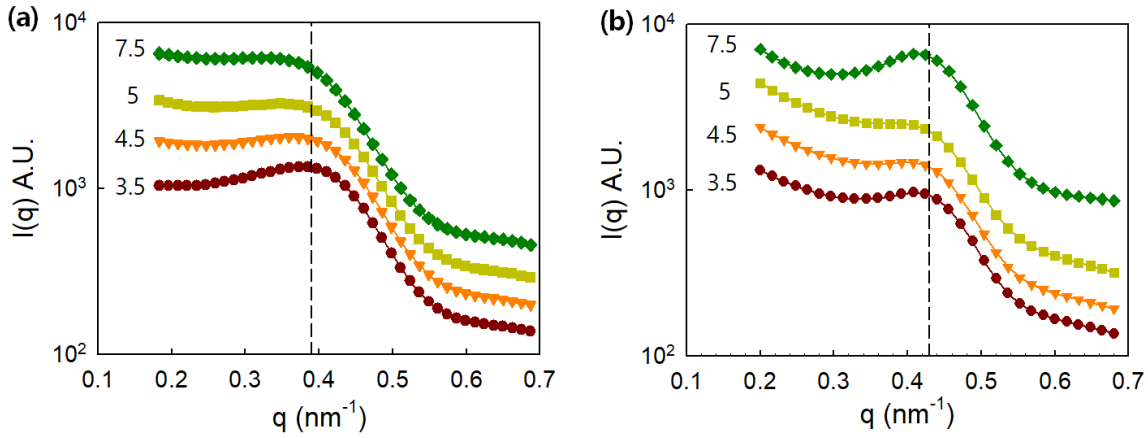

Fig. 6. Small angle x-ray scattering intensity of the silica/PVOH coatings after drying at different pH: (a) pH 3, (b) pH 10. The films were prepared from the aqueous suspension with varying PVOH concentration (wt.%, noted in the figure) and 10 wt.% silica. Dashed lines in (a) and (b) mark the q value of the shoulder intensity of the film (a: q = 0.39 nm^{-1}, b: q = 0.43 nm^{-1})

Stress Development of the Silica/PVOH Coatings During Drying

Stress development of the SiNP-PVOH coating was measured during drying at pH 3 and pH 10 by varying ϕ_{PVOH}. The stress measurement technique allowed not only the ability to quantify the mechanical property of coating layer, but also to understand the solidification behavior of the coating film as the solvent evaporated. Because the SiNP-PVOH coating exhibited a significantly different structure at pH 3 and pH 10, it is worthwhile to characterize the drying behavior and resulting structure and mechanical property, where stress measurement technique plays an important role.

The stress curves of pH 3 and pH 10 are seen in Fig. 7 with respect to ϕ_{PVOH}. The

stress at pH 3 initially rose up to around 50 MPa, and then it abruptly approached a constant value of 45 MPa while it displayed a small peak, as shown in Fig.7a. The stress of pH 10 showed a similar behavior with that of pH 3, but it exhibited a lower peak and constant value, 15 MPa and 10 MPa, respectively, as shown in Fig.7a. It is reported that the peak in the stress curve of the particle-laden coating can be ascribed to the formation of a liquid meniscus among the densely packed particles, where the liquid meniscus induces capillary pressure (Wedin *et al*. 2005). The strength of the capillary pressure was proportional to $2\gamma / r_p$, where γ is the surface tension and r_p is the pore radius, which suggested that small pores in the coating layer resulted in a large stress peak. Therefore, the higher stress increase at pH 3 compared to that at pH 10 could be a result of the formation of smaller pore size than pH 10 in the coating layer, as shown in the SEM image (see ϕ_{PVOH}= 3.5 wt.% in Fig. 5a and 5b).

When ϕ_{PVOH} increased to 4.5 wt.% and 5 wt.%, the level of plateau stress increased for both pHs, but the level at pH 10 more significantly depended on $\phi_{PVOH,}$ as shown in Fig. 7b and 7c. The significant dependence on ϕ_{PVOH} at pH 10 could be explained by the significant change of coating structure, as can be seen in the SEM image (Fig.5b). Pore size was reduced in the SEM image as ϕ_{PVOH} increased, which resulted in a stronger capillary pressure of the meniscus in the pore, and consequently the increased level of stress development. Interestingly, peak signal at pH 3 gradually disappeared, and stress curve showed a longer time to reach the stress plateau as ϕ_{PVOH} increased. This can be explained by the fact that evaporation rate in the polymer phase is much slower than in the particle phase, because solvent evaporation is driven by diffusion in the polymer matrix. Such diffusion is much slower than that in the particle phase, which is driven by capillary flow. Furthermore, it was reported that stress of polymer coating gradually rises without peak during solvent evaporation, which gives rise to a much longer time than that of particle suspensions (Francis *et al*. 2002). Therefore, the reduction of stress peak and longer development time in Fig. 7b and 7c could be explained by the result of increasing contribution of PVOH phase on stress curve.

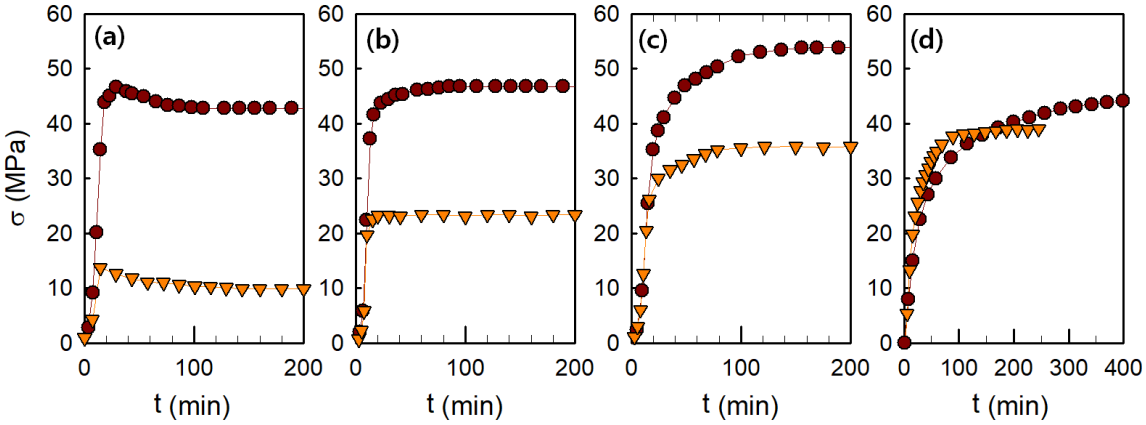

Fig. 7. Stress development of the silica/PVOH coatings of various ϕ_{PVOH}in the coating solution (silica concentration: 10 wt.%) at pH 3(circle) and pH 10(triangle) ϕ_{PVOH} by wt.%: (a) 3.5; (b) 4.5; (c) 5; (d) 7.5

When ϕ_{PVOH} increased to 7.5 wt.%, the stress for pH 10 rose to a plateau stress larger than 5 wt.%, as seen in Fig.7d, owing to the disappearance of pore structure observed at the SEM image(Fig. 5b). On the other hand, stress for pH 3 rose to a plateau stress lower

than 5 wt.%. The observed reduction of stress plateau with the addition of polymer can be found in other particle-polymer coatings (Perera 2004). The authors suggested that mechanical properties of particle-polymer coatings can be classified as 'particle-dominant regime' and 'polymer-dominant regime' as a function of particle/polymer ratio. Particle-dominant regime refers to a mechanically strong coating due to the contribution of inorganic particles, but is brittle due to the lack of polymer. On the other hand, polymer-dominant regime can be defined as a weak coating because of the lack of particles, but it is flexible due to the contribution of continuous polymer phase. Abrupt transition from the particle-dominant regime to the polymer-dominant regime was observed as polymer content increased in the coating layer. Therefore, the reduction of stress plateau observed at ϕ_{PVOH}= 7.5 wt.% could be understood as the coating property shifting into the polymer-dominant regime as PVOH increased.

Structural Development of Silica/PVOH Coatings During Drying

To relate the particle dispersion in the suspension to that in the dried coating at pH 3 and pH 10, respectively, structural development during drying of the suspension was considered.

At pH 3, the clustered structure in the suspension at ϕ_{PVOH} = 3.5 wt.% to 7.5 wt.% became a dense and uniform structure after drying. It should be noted that the SiNP surface was fully saturated by adsorbed PVOH at around ϕ_{PVOH} = 3 wt.%. Therefore, the observed densification of SiNP during drying above ϕ_{PVOH} = 3 wt.% could be attributed to the adsorbed layer, which allowed SiNPs to change their relative position during drying.

At pH 10, a charge-stabilized structure in the suspension became a non-uniform and porous structure after drying, where SiNPs were seriously aggregated. The study on the structural evolution of the SiNPs-PVOH coating at pH 10 showed that phase separation occurred during drying (Kim *et al*. 2016). The mechanism of the phase separation was explained by the depletion flocculation, owing to the lack of polymer adsorption as a consequence of poor particle-polymer interaction.

The observed drying behavior of SiNP-PVOH coatings highlighted the importance of particle-polymer interaction, which enabled control of the SiNPs distribution and corresponding structure and property in SiNP-PVOH coating.

CONCLUSIONS

1. The dispersion stability of the suspension, particle distribution, and mechanical property of dried coating layer in SiNP-PVOH coating were examined, with a focus on the role of physicochemical interaction between particle and polymer.
2. Suspensions of a good interaction at pH 3 and of a poor interaction at pH 10 were selected for comparison, and sedimentation behavior and rheological properties of the suspension were observed by varying PVOH concentration in the suspension. Results showed the dispersion state of SiNPs was strongly dependent on ϕ_{PVOH} at pH 3, whereas dispersion state of charged SiNP at pH 10 was independent of $\phi_{PVOH.}$
3. SEM images and small angle x-ray scattering intensities were probed for the dried SiNP-PVOH coating layer at pH 3 and pH 10. Uniform and dense coating structure with homogeneous SiNP distribution was obtained at pH 3, whereas non-uniform and

porous structure with SiNP aggregates was obtained at pH 10. When ϕ_{PVOH} increased, the distribution of individual SiNPs was further improved at pH 3 as increased PVOH widened SiNP distances. On the other hand, at pH 10, the dispersion of SiNPs inside the aggregates was not improved by increased ϕ_{PVOH}, where PVOH only covered the SiNP aggregates.

4. Stress development during drying was measured by cantilever deflection method to analyze the mechanical property of SiNP-PVOH coating at pH 3 and pH 10. The observed dependency of stress on ϕ_{PVOH} at pH 3 could be explained by the structural change in a spatial arrangement of individual SiNPs in the coating layer. On the other hand, dependency of stress on ϕ_{PVOH} at pH 10 could be explained by the change of the SINP aggregate distribution.

5. In the present study, the dependency of structure and property of SiNP-PVOH coating on ϕ_{PVOH} exhibited a marked difference between the 'good' and 'poor' particle-polymer interaction. These findings relative to a controllable coating structure and property of SiNP-PVOH coating via particle-polymer interaction will provide a useful insight especially in an inkjet coating application, where porosity control is a key-technology for a product performance.

ACKNOWLEDGMENTS

This work was supported by the National Research Foundation of Korea (NRF) grant funded by the Korea government (MSIP) (No.2016R1E1A1A01942362). U-SAXS measurement at beamline 9A, PLS-II was supported in part by MEST and POSTECH.

REFERENCES CITED

Aoki, Y., Hatano, A., and Watanabe, H. (2003). "Rheology of carbon black suspensions. I. Three types of viscoelastic behavior," *Rheol. Acta* 42(3), 209-216. DOI: 10.1007/s00397-002-0278-3

Bansal, A., Yang, H., Li, C., Cho, K., Benicewicz, B. C., Kumar, S. K., and Schadler, L. S. (2005). "Quantitative equivalence between polymer nanocomposites and thin polymer films," *Nat. Mater.* 4,693-698. DOI: 10.1038/nmat1447

Chang, H., Tu, K., Wang, X., and Liu, J. (2015). "Facile preparation of stable superhydrophobic coatings on wood surfaces using silica-polymer nanocomposites," *BioResources* 10(2), 2585-2596. DOI: 10.15376/biores.10.2.2585-2596

Chen, Y., Jiang, B., Liu, L., Du, Y., Zhang, T., Zhao, L., and Huang, Y. (2017). "High ink absorption performance of inkjet printing based on SiO_2@Al_{13}core-shell composites," *Appl. Surf. Sci.*436, 995-1002.DOI: 10.1016/j.apsusc.2017.12.071

Ching, Y. C., Rahman, A., Ching, K. Y., Sukiman, N. L., and Cheng, H. C. (2015). "Preparation and characterization of polyvinyl alcohol-based composite reinforced with nanocellulose and nanosilica," *BioResources* 10(2), 3364-3377. DOI: 10.15376/biores.10.2.3364-3377

Corcoran, E. M. (1969). "Determining stresses in organic coatings using plate beam deflection," *J. Paint Technol.* 41(538), 635-640.

Francis, L. F., Mccormick, A. V., Vaessen, D. M., and Payne, J. A. (2002). "Development and measurement of stress in polymer coatings," *J. Mater. Sci.* 37(22), 4717-4731. DOI: 10.1023/a:1020886802632

Di Giuseppe, E., Davaille, A., Mittelstaedt, E., and François, M. (2012). "Rheological and mechanical properties of silica colloids: From Newtonian liquid to brittle behaviour," *Rheologica Acta* 51(5), 451-465. DOI: 10.1007/s00397-011-0611-9

Hatakeyama, T., Ikeda, Y., and Hatakeyama, H. (1987). "Effect of bound water on structural change of regenerated cellulose," *Macromol. Chem. Phys.* 188(8), 1875-1884. DOI:10.1002/macp.1987.021880811

Jouault, N., Zhao, D., and Kumar, S. K. (2014). "Role of casting solvent on nanoparticle dispersion in polymer nanocomposites," *Macromolecules* 47(15), 5246-5255. DOI: 10.1021/ma500619g

Kim, S., Hyun, K., Kim, Y. S., Struth, B., Clasen, C., and Ahn, K. H. (2013). "Drying of a charge-stabilized colloidal suspension *in situ* monitored by vertical small-angle x-ray scattering," *Langmuir* 29(32), 10059-10065. DOI: 10.1021/la401897n

Kim, S., Hyun, K., Moon, J. Y., Clasen, C., and Ahn, K. H. (2015). "Depletion stabilization in nanoparticle-polymer suspensions: Multi-length scale analysis of microstructure," *Langmuir* 31(6), 1892-1900. DOI: 10.1021/la504578x

Kim, S., Hyun, K., Struth, B., Ahn, K. H., and Clasen, C. (2016). "Structural development of nanoparticle dispersion during drying in polymer nanocomposite films," *Macromolecules* 49(23), 9068-9079. DOI:10.1021/acs.macromol.6b01939

Kim, S., Sung, J. H., Ahn, K. H., and Lee, S. J. (2009). "Drying of the silica/PVOH suspension: Effect of suspension microstructure," *Langmuir* 25(11), 6155-6161. DOI: 10.1021/la804112b

Kim, S., Sung, J. H., Hur, K., Ahn, K. H., and Lee, S. J. (2010). "The effect of adsorption kinetics on film formation of silica/PVOH suspension," *J. Colloid Interface Sci.* 344(2), 308-314. DOI: 10.1016/j.jcis.2009.12.046

Koo, O. M. Y., Fiske, J. D., Yang, H., Nikfar, F., Thakur, A., Scheer, B., and Adams, M. L. (2011). "Investigation into stability of poly(vinyl alcohol)-based opadry® IIfilms," *AAPS PharmSciTech* 12(2),746-754. DOI: 10.1208/s12249-011-9630-1

Lamminmäki, T. T., Kettle, J. P., Puukko, P. J. T., Ridgway, C. J., and Gane, P. A. C. (2012). "Short timescale inkjet ink component diffusion: An active part of the absorption mechanism into inkjet coatings," *J. Colloid Interface Sci.* 365(1), 222-235. DOI:10.1016/j.jcis.2011.08.045

Lee, J., Sung, S., Kim, Y., Park, J. D., and Ahn, K. H. (2017). "A new paradigm of materials processing - Heterogeneity control," *Curr. Opin. Chem. Eng.* 16, 16-22. DOI:10.1016/j.coche.2017.04.002

Nasser, M. S., Al-Marri, M. J., Benamor, A., Onaizi, S. A., Khraisheh, M., and Saad, M. A. (2016). "Flocculation and viscoelastic behavior of industrial papermaking suspensions," *Korean J. Chem. Eng.* 33(2), 448-455. DOI: 10.1007/s11814-015-0167-y

Otsubo, Y. (1986). "Effect of polymer adsorption on the rheological behavior of silica suspensions," *J. Colloid Interface Sci.* 112(2), 380-386. DOI: 10.1016/0021-9797(86)90105-0

Payne, J. A., McCormick, A. V., and Francis, L. F. (1997). "*In situ* stress measurement apparatus for liquid applied coatings," *Rev. Sci. Instrum.* 68(12), 4564-4568. DOI: 10.1063/1.1148432

Perera, D. Y. (2004). "Effect of pigmentation on organic coating characteristics," *Prog.*

Org. Coat. 50(4), 247-262. DOI:10.1016/j.porgcoat.2004.03.002

Pingan, H., Mengjun, J., Yanyan, Z., and Ling, H. (2017). "A silica/PVOH adhesive hybrid material with high transparency, thermostability and mechanical strength," *RSC Adv.* 7(5), 2450-2459. DOI: 10.1039/c6ra25579e

Ribeiro, T., Baleizão, C., and Farinha, J. P. (2014). "Functional films from silica/polymer nanoparticles," *Materials* 7(5), 3881-3990. DOI: 10.3390/ma7053881

Su, L., Xing, Z., Wang, D., Xu, G., Ren, S., and Fang, G. (2013). "Mechanical properties research and structural characterization of alkali lignin / poly(vinyl alcohol) reaction films," *BioResources* 8(3), 3532-3543. DOI: 10.15376/biores.8.3.3532-3543

Tadros, T. F. (1978). "Adsorption of polyvinyl alcohol on silica at various pH values and its effect on the flocculation of the dispersion," *J. Colloid Interface Sci.* 64(1), 36-47. DOI: 10.1016/0021-9797(78)90332-6

Tummala, G. K., Rojas, R., and Mihranyan, A. (2016). "Poly(vinyl alcohol) hydrogels reinforced with nanocellulose for ophthalmic applications: General characteristics and optical properties," *J. Phys. Chem. B* 120(51),13094-13101. DOI: 10.1021/acs.jpcb.6b10650

Wedin, P., Lewis, J. A., and Bergström, L. (2005). "Soluble organic additive effects on stress development during drying of calcium carbonate suspensions," *J. Colloid Interface Sci.* 290(1), 134-144. DOI: 10.1016/j.jcis.2005.04.020

Yang, J.-M., Wang, N.-C., and Chiu, H.-C. (2014). "Preparation and characterization of poly(vinyl alcohol)/sodium alginate blended membrane for alkaline solid polymer electrolytes membrane," *J. Membr. Sci.* 457,139-148. DOI: 10.1016/j.memsci.2014.01.034

Zhang, Y., Liu, Z., Cao, Y., Li, R. A., and Jing, Y. (2015). "Impact of binder composition on inkjet printing paper," *BioResources* 10(1), 1462-1476. DOI: 10.15376/biores.10.1.1462-1476

Zou, H., Wu, S., and Shen, J. (2008). "Polymer/silica nanocomposites: Preparation, characterization, properties, and applications," *Chem. Rev.* 108(9), 3893-3957. DOI: 10.1021/cr068035q

Article submitted: January 18, 2018; Peer review completed: February 26, 2018; Revised version received and accepted; March 6, 2018; Published: March 13, 2018.
DOI: 10.15376/biores.13.2.3195-3207